Journal of Structural Geology, Vol. 15, No. 2, pp. 177 to 189, 1993
Printed in Great Britain

0191-8141/93 $06.00+0.00
© 1993 Pergamon Press Ltd

Magmatic strains and foliation triple points of the Merrimac plutons, northern Sierra Nevada, California: implications for pluton emplacement and timing of subduction

GIOVANNI GUGLIELMO, JR*

Earth Sciences Board, University of California, Santa Cruz, CA 95064, U.S.A.

(*Received* 10 *October* 1991; *accepted in revised form* 21 *July* 1992)

Abstract—Cross-cutting relationships between regional structures and post-tectonic plutons of known age are commonly used to date regional deformation in orogenic belts. In order to show that a pluton is post-tectonic one must demonstrate that the strains within the pluton are not due to regional tectonic processes. This paper reports strain measurements associated with pluton emplacement in northern Sierra Nevada. These strain data and a microstructural analysis indicate that strains within the Merrimac plutons are due to igneous not tectonic processes, which strengthens the hypothesis that the plutons were emplaced after the formation of regional structures and mélanges. Radiometric ages of the Merrimac pluton, in concert with structural data, place a more reliable upper Jurassic limit on the age of the subduction in the Western Belt of northern Sierra Nevada. This paper also reports constrictional strains around plutons, and suggests that the Merrimac plutons contributed significantly to the ductile strains observed in the wall rocks.

INTRODUCTION

PLUTON emplacement contributes to the complexity of structures observed in orogenic belts because these structures commonly form by interactions between regional tectonic and local pluton-related strain fields. Plutons contribute to country rock deformation by generating strain fields during their ascent and expansion, and they facilitate deformation by increasing the regional temperature and amount of fluids, consequently softening the wall rocks (Marsh 1982, Etheridge *et al.* 1983, Tobisch *et al.* 1986, Barton & Hanson 1989). The type, orientation and intensity of these structures depend on several variables related to pluton emplacement, such as: (1) the number, sequence, rates and duration of multiple episodes of pluton- and tectonic-related deformation; and (2) interactions among strain fields produced by multiple intrusions of plutons. The extent to which pluton-related strains control structures in orogenic belts remains an unanswered question. Furthermore, cross-cutting relations between regional structures and post-tectonic plutons of known age are commonly used to place upper limits on the age of regional deformation. In order to show that a pluton is post-tectonic one must demonstrate that the strains within the pluton are not due to tectonic processes.

This paper is part of a study that integrates field, laboratory and theoretical aspects of pluton emplacement, and reports strain measurements within and around the Merrimac nested plutons in northern Sierra Nevada, California (Fig. 1). The comparison between strain measurements presented herein, with compositional, structural (Guglielmo in press b) and three-dimensional numerical modeling studies (Guglielmo 1992, in press a,c) provide insights to the relative contribution of pluton-related deformation for the structures measured in orogenic belts. In addition, these measurements, when analyzed together with microstructural data, show that the foliation within the Merrimac plutons is magmatic and that the plutons were probably emplaced after the formation of regional structures. Therefore, U/Pb ages from the Merrimac plutons provide a minimum age for the Jurassic (?) subduction that presumably formed mélanges in northern Sierra Nevada.

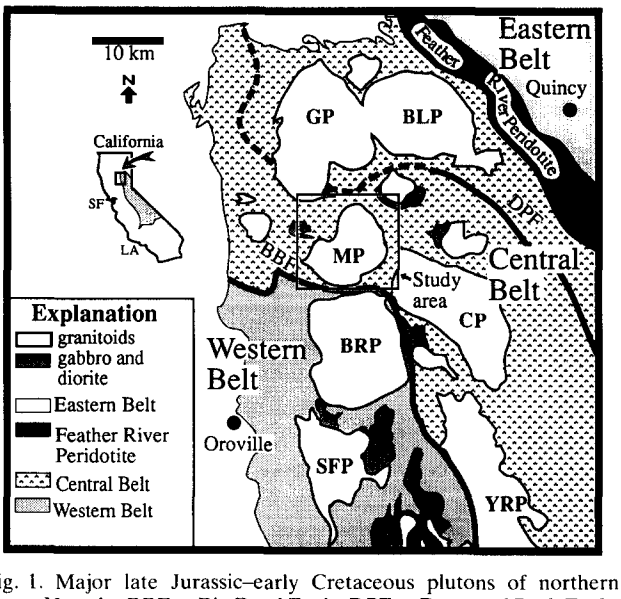

Fig. 1. Major late Jurassic–early Cretaceous plutons of northern Sierra Nevada. BBF = Big Bend Fault, DPF = Dogwood Peak Fault, BLP = Bucks Lake, BRP = Bald Rock, CP = Cascade, GP = Grizzly, MP = Merrimac, SFP = Swedes Flat, and YRP = Yuba River. (Simplified after Jennings *et al.* 1973, Day *et al.* 1985, 1988 and Dilek *et al.* 1991.)

*Current address: Department of Geological Sciences, University of California, Santa Barbara, CA 93106, U.S.A.

REGIONAL GEOLOGY

Concentric composition patterns and cross-cutting foliation patterns within the Merrimac body suggest that this body is composed of two tonalitic–granodioritic plutons (Guglielmo in press b). These plutons are part of a Cretaceous–Jurassic granitoid suite that intrudes the Central Belt of northern Sierra Nevada (Fig. 1).

This belt includes all the rocks west of the Feather River Peridotite Belt and east of the Western Belt. Although stratigraphically complex, the Central Belt is composed of three major units: (1) late Paleozoic–early Mesozoic metasedimentary and metavolcanic rocks of the Calaveras Complex (Schweickert 1978, Sharp 1988); (2) late Paleozoic(?)–early Mesozoic ophiolitic assemblages and mélange terranes overlain by hemipelagic sedimentary rocks (Fiddle Creek complex of Edelman *et al.* 1989, Jarbo Gap ophiolite of Dilek 1989, Dilek *et al.* 1991); and (3) early Jurassic volcano-plutonic arc sequence of the Slate Creek complex (Day *et al.* 1985, Bickford & Day 1988, Edelman *et al.* 1989). The Merrimac plutons intrude unit (2), which corresponds to parts of the Horseshoe Bend Formation (Hietanen 1951, 1973, 1976, 1981) and the Tuolumne River Terrane (Edelman & Sharp 1989). These rocks have been tightly folded, overturned, faulted and metamorphosed up to greenschist facies to lower amphibolite (Hietanen 1973, 1976, Day *et al.* 1988, Dilek, 1989) and are interpreted as an ophiolitic mélange (Schweickert & Cowan, 1975, Edelman & Sharp 1989). Rocks within the Central Belt as a whole have a steeply dipping NNW cleavage commonly attributed to the late Jurassic Nevadan orogeny (Taliaferro 1942, Bateman & Clark 1974, Clark 1976, Mazaheri 1982, Schweickert *et al.* 1984, Murphy & Moores 1985, Murphy 1986, Dilek 1989, Edelman *et al.* 1989, Edelman & Sharp 1989, Dilek *et al.* 1991). Within the study area, foliation trends and compositional layering are predominantly steeply dipping and wrap around the Merrimac plutons. The plutons are bordered by the Dogwood Peak and unnamed faults to the north and by the Big Bend fault zone to the south (Fig. 1). These faults apparently bend around but do not cut the pluton. Hietanen (1951, 1973, 1976, 1981) and Clark (1976) argued that the Merrimac body is a post-tectonic, forcibly-emplaced pluton that bent these earlier NW structural trends. However, recent work (Paterson & Tobisch 1988) has shown that faults and foliations may also bend around pre-tectonic plutons. In addition, it is difficult to determine whether structures around most plutons are produced by pluton emplacement or by tectonic deformation. Therefore, the timing relationship between the Merrimac plutons and the surrounding major faults remains unclear.

Age of the plutons

K/Ar ages for the northern Merrimac pluton were determined on biotite as 131 Ma and on hornblende as 129 Ma (Grommé *et al.* 1967). Preliminary U/Pb ages (M. Martin and J. D. Walker personal communication 1991) suggest that both plutons, although structurally and compositionally distinct, belong to the same magmatic event (Guglielmo in press b). Zircon separates from two samples yielded concordant ages of 142 ± 3 Ma for the northern Merrimac pluton, and discordant ages of 142 ± 3 Ma for the southern Merrimac pluton.

STRAIN MEASUREMENTS

Limitations of enclaves as strain markers

Shape ratios of microgranitoid enclaves (Balk 1937, Escorza 1978, Holder 1979, Ramsay & Huber 1983, Ramsay 1989) were used to estimate strains within the Merrimac plutons. Although there are limitations to the interpretation of strains obtained from individual enclaves, their map-scale patterns and trends provide useful information on the emplacement history of the plutons.

The interpretation of total strains measured in enclaves has to be done with care because several interrelated variables, other than kinematics of pluton emplacement, affect the strain recorded by individual microgranitoid enclaves. For example, the initial shapes of enclaves may not be spheres. Both spherical and elliptical microgranitoid enclaves can be incorporated into a magma chamber during magma mingling events, increasing the variety of shapes in the enclaves' population (Vernon *et al.* 1988).

In addition, absolute viscosity and viscosity contrasts between enclave and matrix, as well as viscosity variations in time and space within the magma chamber will affect the strain recorded by the enclaves. Viscosity, in turn, depends on crystal content, composition, temperature, fluid pressure of the matrix and of the enclave, and strain rates (Shaw 1965, Bottinga & Weill 1972, Brandeis & Marsh 1989). Differential stresses caused by viscous dragging during rising of the pluton (Cruden 1988, 1990, Schmeling *et al.* 1988) as well as tectonic stresses can also contribute to enclave strain. This complex interplay of variables complicates our interpretation of the strain recorded by the enclaves.

Viscosity contrasts between strain marker and matrix largely control the strain history of the marker. The higher the viscosity contrast between strain marker and matrix, the less is the ability of the marker to change shape. Therefore, enclaves may preferentially record periods of the matrix strain history when the contrast difference between enclave and matrix was low. Consequently, strain measurements in individual enclaves will underestimate the total strain undergone by the matrix.

In addition to viscosity contrast, *absolute viscosities* of both enclave and matrix affect strain in the enclaves. At high absolute matrix viscosities, the matrix can effectively transmit stresses to deform strain markers. These high matrix viscosities are expected at final stages of magma chamber crystallization. Therefore, the strain measured in enclaves will preferentially record the final stages of pluton emplacement, and the total strains in

the enclave will, again, underestimate the strains undergone by the matrix.

Furthermore, *viscosity changes* in three-dimensional space can unpredictably affect strain in the enclaves. During static progressive crystallization of the magma, the margins of the magma chamber solidify first. This differential crystallization generates viscosity gradients, where viscosities in the margins of the magma chamber are higher than viscosities in the center. Therefore, enclaves at the margin of the pluton will experience higher differential stresses and resulting total strains than enclaves at the center. Viscosity changes also occur over time. Differential stress distribution within the magma chamber will change as crystallization proceeds. Regions of differential stresses at the margins of the pluton will progressively grow, whereas regions of hydrostatic stresses at the center shrink. This inhomogeneous stress field in space and time further complicates the strain history recorded in the enclaves. However, despite limitations, microgranitoid enclaves have provided useful insights on strain patterns present within plutons (Ramsay 1975, 1989, Holder 1979, Hutton 1982, Lagarde & Choukroune 1982, Courrioux 1987).

Strain measurements within the Merrimac plutons

Weathering of rocks in the Merrimac plutons facilitated strain measurements in enclaves at 15 sites. In most outcrops, granitoid and enclaves are either friable or soft enough that they can be sliced with a shovel or carved with a rock pick. Visualization of the approximate three-dimensional shape of the enclave and subsequent direct measurement of its principal axes was accomplished by two methods. The first method involved cutting the granitoid along two perpendicular planes, both of which are perpendicular to the foliation. This procedure works well for enclaves of flattening type. However, it requires constant monitoring of the curvatures of the margin of the enclave during cutting to assure that final slices pass through the center of the enclave. The second method involved gradually carving the enclave out of the granite, which destroys the enclave but leaves a cavity in the granite that preserves its approximate shape.

Strains within the Merrimac plutons were calculated by the geometric mean of the ellipticity of enclaves measured at each locality (as in Dunnet 1969, Lisle 1977, Ramsay 1989). Differences in ellipticity resulting from using geometric instead of harmonic means are irrelevant compared with errors inherent to using enclaves as strain markers described above. Typically between five and 10 enclaves were available for measurement at each site. Errors involved in strain measurements and strain analyses were acceptable because in most cases the foliation within the Merrimac plutons is not deflected by the enclaves, which suggests that viscosity contrasts between matrix and markers were not high at the time of foliation development. However, limitations inherent to the use of enclaves as strain markers imply that absolute strain values at each locality are less significant than strain gradients and patterns viewed in map scale.

Strain measurements in the wall rock

Strain samples in the wall rock included clasts in melanges and in marble breccias. Eight oriented samples were analyzed. Three perpendicular cuts were made through each sample. For each cut, a R_f/ϕ file containing the lengths of the major and minor axis of each clast, as well as the orientation of the major axis was compiled. Subsequently, these files were input to programs that follow the techniques of Shimamoto & Ikeda (1976), Lisle (1977) and Miller & Oertel (1979) to calculate the lengths and orientations of the axes of three-dimensional strain ellipsoids. Strain intensities were calculated using the formula of Nadai (Nadai 1963), and shapes were calculated using Lode's parameter (Lode 1926). These data are shown in Figs. 2–6.

It is assumed that the original, undeformed, clasts were ellipsoidal and randomly oriented. It is also assumed that the clasts deform homogeneously with the matrix at constant volume. Sources of errors in strain measurements in the wall rock around the Merrimac plutons included the small number of suitable markers and variations in rock type between different localities. In addition, errors in strains measured at each locality are expected due to variable viscosity contrasts between clast and matrix as well as the presence of primary fabrics. Despite these limitations, the available markers outlined useful map-view strain trends.

In this paper, the words 'ends of the pluton' refer to the wall rock located east and west of each pluton. Conversely, 'sides of the pluton' refer to the north and south of each pluton (Fig. 2). Strain measurements in the wall rock show that orientation and shape of strain ellipsoids on the sides of the pluton are different from trends at the ends of the pluton. At the sides of the pluton, strain shapes are oblate, with Lode's parameters ranging from 0.45 to 0.52 (Figs. 3 and 4), and strain intensity values range from of 0.85 to 1.08 (Figs. 4 and 5). Foliations, and xy planes of strain ellipsoids, are parallel to the margins of the pluton (Figs. 2 and 6). At the ends of the pluton, strain ellipsoids are largely prolate to plane, with Lode's parameter between -0.15 and 0.08 (Figs. 3 and 4), and strain intensities in the wall rock range from 0.75 to 1.43 (Figs. 4 and 5). Most significantly, the foliation forms four triple points.

ORIGINS OF STRAIN WITHIN THE MERRIMAC PLUTONS

The origin of strain within plutons is usually controversial and difficult to determine (e.g. Paterson *et al.* 1989). Strain recorded by enclaves could be a result of (1) *igneous* processes such as magmatic flow (Berger & Pitcher 1970, Marre 1987) or pluton expansion in the solid state (Ramsay 1989); (2) *tectonic* deformation (Paterson *et al.* 1987); or (3) a combination of the two.

Microstructures and strains patterns can provide insight to the origin of the strain within the Merrimac plutons.

Foliation is defined by aligned euhedral crystals of plagioclase, hornblende and biotite (Fig. 7). Microstructures include hypidiomorphic-granular and granophyric textures. Virtually no evidence of solid-state deformation is found within the bulk of the plutons. Evidence for solid-state deformation in the crystals of the granite and of the enclaves is scant, and is only found within the first 10 m or so from the contact. Microstructures within the zone of solid-state deformation include undulatory extinction and subgrain development in quartz, bending of biotite and rare (one grain found in 52 large thin sections) fractured plagioclase (Fig. 7).

Strain ellipsoids calculated within both plutons show nearly perfect oblate shapes (Figs. 3 and 4) and concentric patterns of long axes of strain ellipsoids (Figs. 2 and 6a). In addition, strain intensities within the southern pluton increase toward the margin of the pluton (Fig. 5).

One could argue that enclaves were strained in the solid state and microstructures recording this deformation were erased by subsequent recrystallization. However, mineral assemblages that form the foliation in the granite are similar to the assemblages in the enclaves; only the mineral proportions are different. Therefore, if solid-state deformation or recrystallization affected the enclaves, it should have affected the crystals that make up the foliation within the granite. Crystals in the granite are euhedral. Therefore the granite and the enclaves were neither deformed in the solid state nor recrystallized.

A magma mush with less than 70% crystals is incapable of recording solid-state deformation (Van der Molen & Paterson 1979). Therefore, the lack of solid-state deformation within the Merrimac plutons suggests that strain and microstructures were produced by magma flow while the plutons were incompletely crystallized. In a partially crystallized magma chamber, the resulting magma viscosities could be high enough to transmit differential stresses to change the shape of unconsolidated crystal aggregates, such as mafic enclaves, but not enough to imprint solid-state fabrics within crystals in the granite or in the enclaves.

Each of the strain map patterns by itself does not offer unequivocal proof of igneous origin for the strain. However, viewed in *combination*, and analyzed in concert with magmatic microstructures, these strain patterns, especially concentric pattern of strain ellipsoids within a circular pluton, are unlikely to be the result of tectonic deformation. Therefore, strains within the pluton were caused by igneous processes.

Pluton expansion

Ramsay (1989) demonstrated that the Chindamora batholith was built by successive rises of magmatic

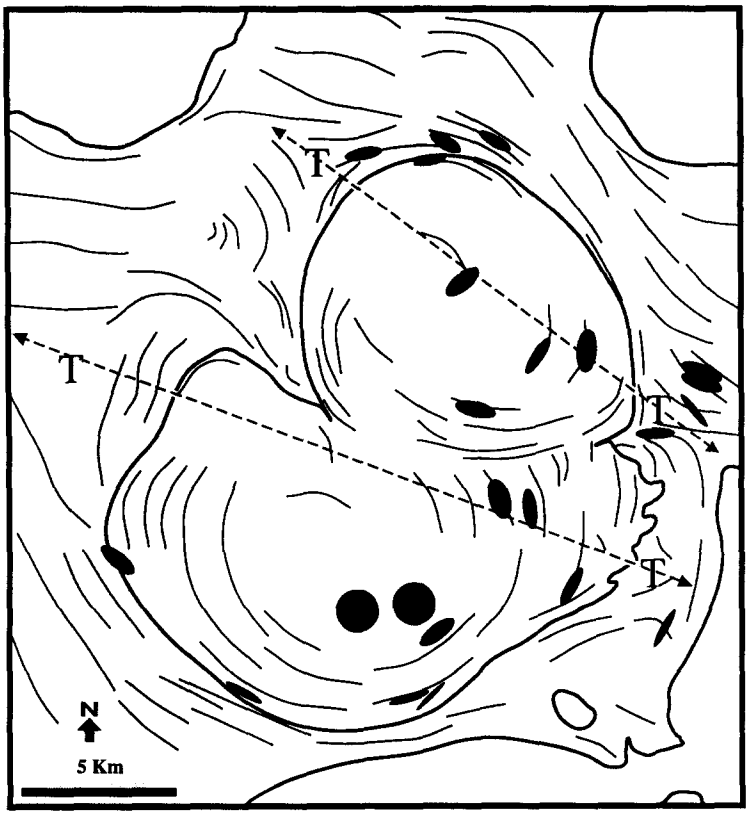

Fig. 2. Map of *XZ* ellipses and trends of foliation. Strain markers were microgranitoid enclaves within the pluton and clastic rocks in the country rock (see text). Within the pluton, strain ellipses form concentric patterns, *Z* axes are subhorizontal (Fig. 6a), and strains are mostly of ideal flattening type (Fig. 4). Therefore, the strike of the axes of the *XZ* ellipses gives the orientation of the axes of the strain ellipsoid within the pluton. Foliations trends (continuous lines) of the northern pluton intersect the ones in the southern pluton. Country rock foliation wraps around the plutons. Foliation triple points (T) at the ends of each pluton follow a NW trend (dashed lines).

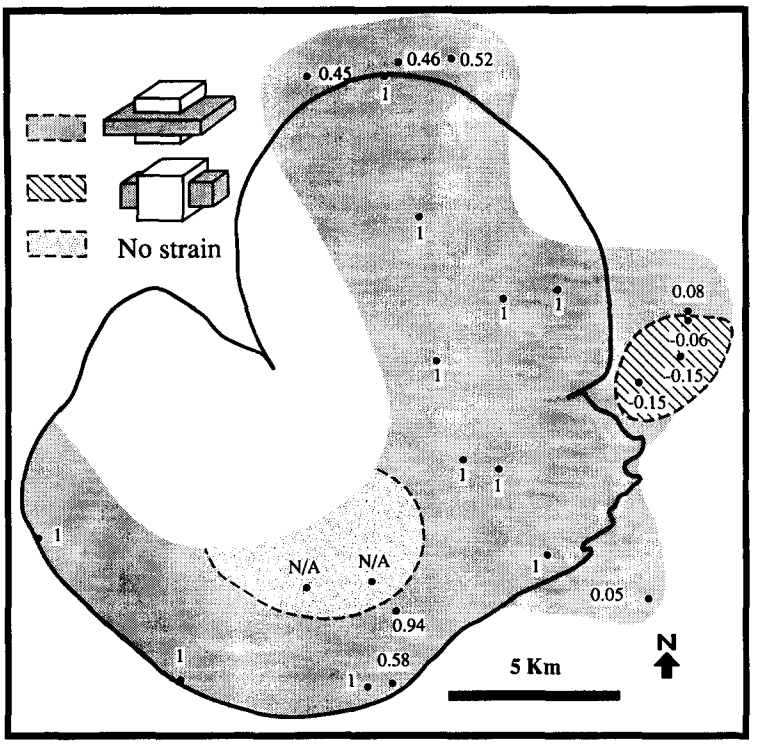

Fig. 3. Map of strain ellipsoid shapes as defined by Lode's parameter (Lode 1926)

$$\nu = \frac{2\varepsilon_2 - \varepsilon_1 - \varepsilon_3}{\varepsilon - \varepsilon_3},$$

where ε_1, ε_2 and ε_3 are principal logarithmic strains given by

$$\varepsilon_1 = \ln(1 + e_1); \quad \varepsilon_2 = \ln(1 + e_2) \quad \text{and} \quad \varepsilon_3 = \ln(1 + e_3),$$

where $(1 + e_1)$, $(1 + e_2)$ and $(1 + e_3)$ are the lengths of the strain ellipsoid semi-axes and e_1, e_2 and e_3 are the values of principal strains. Lode's parameter assumes values between -1 and 1, where negative values represent constriction and positive values represent flattening. Lode's parameter equal to zero represents plane strain. Lode's parameters are non-applicable (N/A) in areas of no strain. Notice: (1) flattening values at the sides of the northern pluton; (2) constrictional values eastern of the northern pluton; and (3) flattening within both plutons.

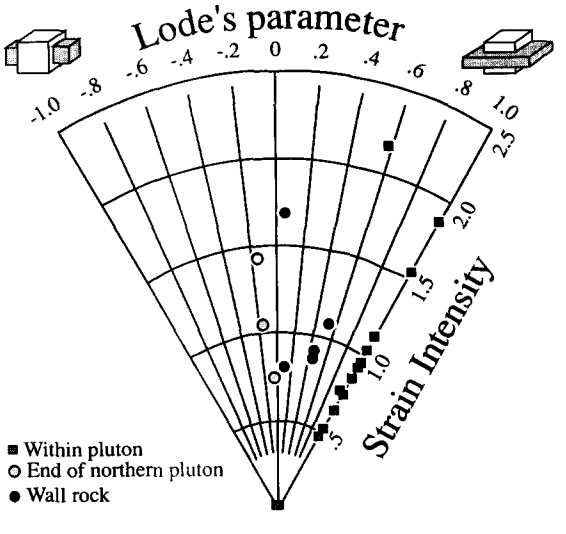

Fig. 4. Hsu diagram (Hsu 1966) of strain intensity and shape. Strain magnitude (Nadai 1963) is given by:

$$\bar{\varepsilon}_s = \frac{1}{\sqrt{3}}((\varepsilon_1 - \varepsilon_2)^2 + (\varepsilon_2 - \varepsilon_3)^2 + (\varepsilon_3 - \varepsilon_1)^2)^{1/2}.$$

Notice: (1) a wide range of strain magnitudes within the pluton (squares), where strains' intensities range from 0 to 2.17; (2) moderate constrictional strains at the ends of the northern pluton (gray circles) and moderate to high strains in the wall rock (solid circles).

pulses about a common center. Each pulse caused stretching of previously crystallized rock. This solid-state pluton 'ballooning' would have produced (1) concentric patterns of flattening strains whose approximate intensity increase from the center towards the margin of the pluton, and (2) conjugate ductile shear zones defining concentric directions of maximum extension.

In this paper I use the word *expansion* as alternative to ballooning. Expansion describes an increase in radius of the pluton. This increase can be of any amount, may occur in the liquid or solid state, and is not necessarily uniform in all directions. Estimates of wall rock shortening, obtained from measured ductile strains would, necessarily, underestimate the room required for emplacement of the Merrimac plutons, therefore these estimates were not calculated. Such estimates would not account for pluton-related strains far from the pluton. These distal strains are small and, therefore, difficult to measure accurately. In a ductile crust, distal strains may affect three-dimensional regions larger than the pluton itself (e.g. Dixon 1975, Cruden 1990). Therefore, although of small magnitude at each locality, the sum of these strains account for large portions of the space required for pluton emplacement. In addition, distal *and* proximal strains are distorted by interferences with

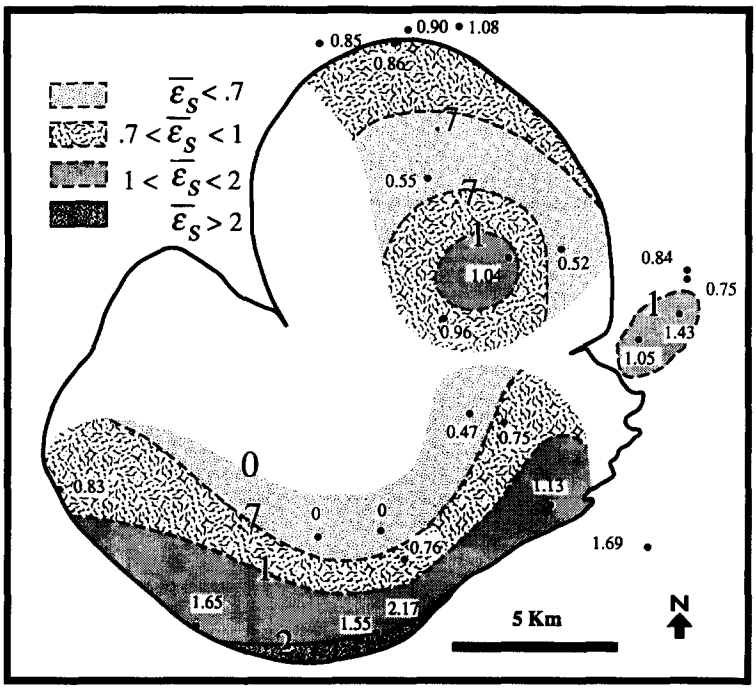

Fig. 5. Strain magnitude map. The southern pluton strain magnitudes ($\bar{\varepsilon}_s$) are zero at the center and progressively increase toward the margin, whereas within the northern pluton the highest strain are in the center. Strains at the end of the northern pluton are unusually high.

neighboring plutons and tectonic deformation. Furthermore, any space for the pluton made by expansion would be underestimated, because wall rock ductile strains would not record part of the room for the pluton that was made by an undetermined amount of stoping.

With exception of strains in the center or the northern pluton, map view patterns of strain ellipsoid intensity, orientation and shape within the Merrimac plutons are consistent with ballooning. However, no discrete shear zones and only scant solid-state deformation were observed along the margins of the plutons. Furthermore, as described above, microstructural evidence within both Merrimac plutons away from their boundaries shows no evidence of solid-state deformation, such as recrystallization or plastic deformation, within the crystals, either within the enclaves or matrix. Therefore, expansion in the Merrimac plutons could not have happened in the solid state. Strains within each of the Merrimac plutons are consistent with, but do not prove, that these plutons expanded. In addition, if expansion happened, it was not equal in all directions. For example, the discordant contact between the northern and southern Merrimac plutons suggests that the northern Merrimac pluton did not ductily deform its wall rock to the south by expansion or by any other means.

CENTRIFUGE AND NUMERICAL MODELS

Comparison between strain measurements within and around the Merrimac plutons and strains obtained from centrifuge and numerical models aids in analyzing poss-

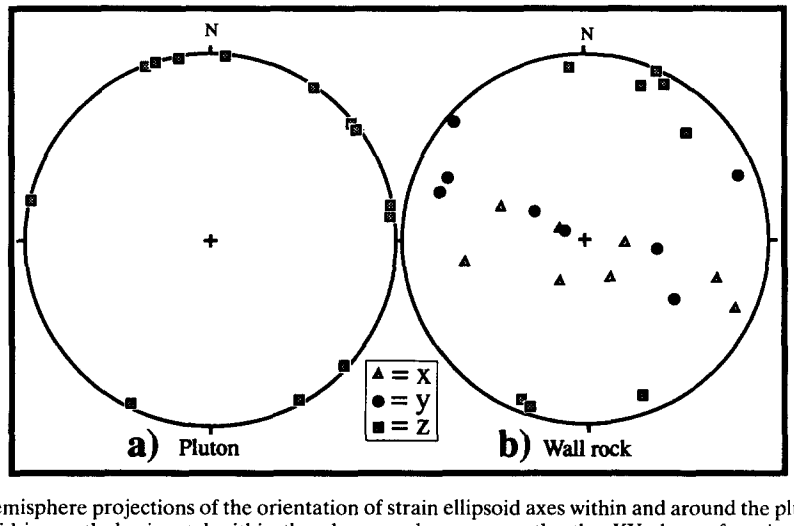

Fig. 6. Lower-hemisphere projections of the orientation of strain ellipsoid axes within and around the pluton. (a) Z axis of the strain ellipsoid is mostly horizontal within the pluton and, consequently, the XY plane of strain ellipsoid is nearly vertical. Orientations of X and Y axis are not significant within the pluton because strains are mostly of flattening type. (b) Z axes are also mostly horizontal within the wall rock.

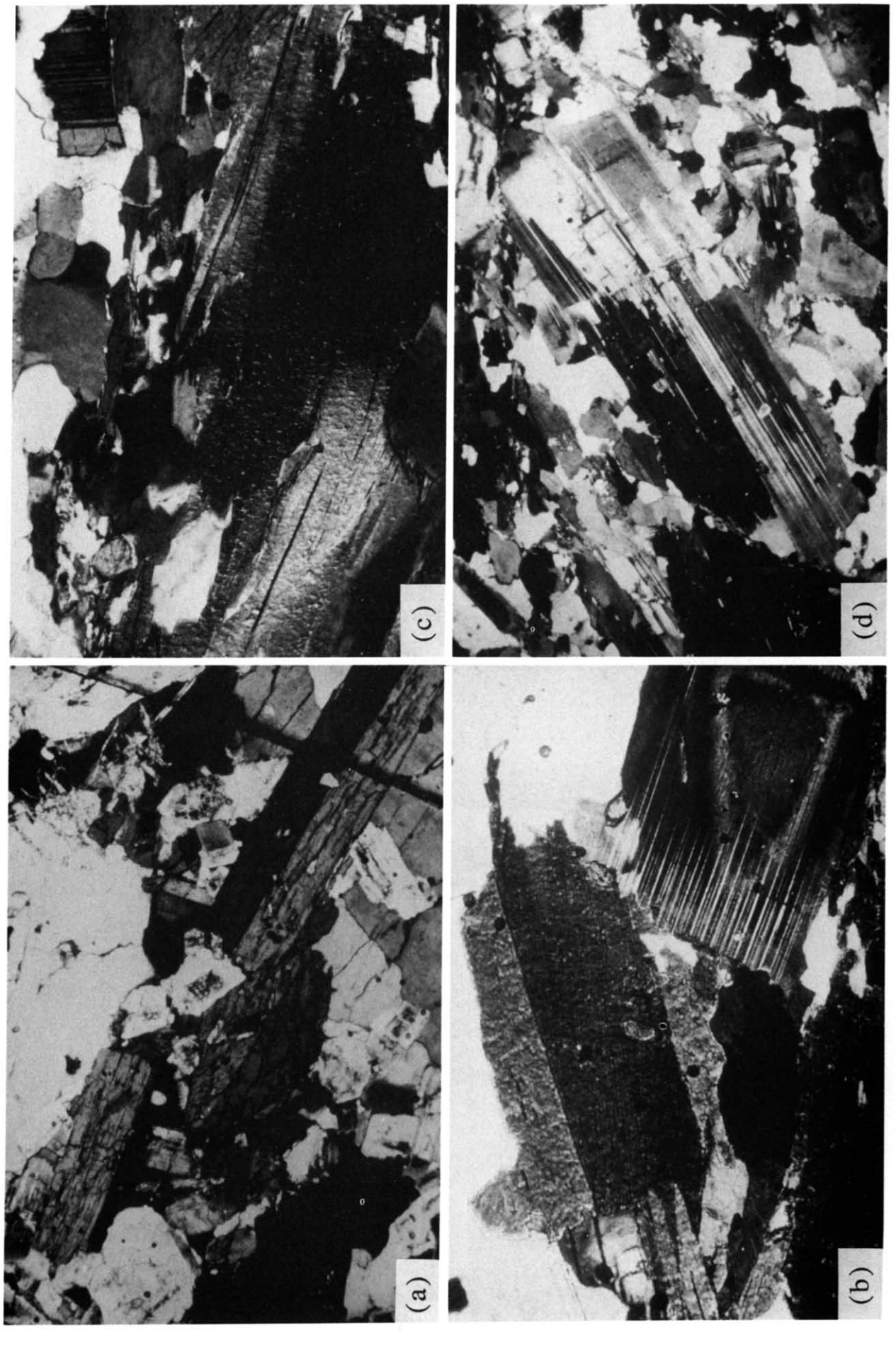

Fig. 7. Microstructures defining the foliation within the Merrimac plutons. Foliation is dominantly magmatic as shown by (a) euhedral hornblende as well as (b) unkinked biotite, zoned plagioclase and undeformed quartz. Solid-state deformation is scant as shown by (c) the most kinked biotite, and (d) the only broken feldspar crystal found within the pluton.

ible origins of strains within and around the plutons. Models also suggest the approximate level at which the pluton is presently exposed. This is useful because pluton contacts and foliation are nearly vertical, which hinder reconstruction of the three-dimensional shape of the pluton from map data.

Centrifuge 'clay' models are helpful in describing the flow patterns and processes associated with diapiric emplacement (Ramberg 1970, 1972, 1981, Talbot 1974, 1977, Schwerdtner *et al.* 1977, Soula 1982, Jackson & Talbot 1989, Koyi 1991). In addition, some models actually quantify strains expected within and around the pluton (Dixon 1975, Schwerdtner & Troeng 1978, Cruden 1988, 1990). Although these models are simplified approximations of natural plutons, i.e. emplaced in isothermal conditions, are made of silicon putty, and are not subjected to tectonic deformation, they give insights to the possible causes of strains measured within and around the Merrimac plutons.

Dixon (1975) simulated strains associated with the emplacement of a diapiric ridge that is more viscous than the wall rock (Fig. 8a). His model corresponds to an immature pluton that rises a short distance within the crust. Although these conditions may or may not apply to the Merrimac plutons, Dixon's model is one of the few that quantifies strain patterns and therefore is worth using. Dixon's models are two-dimensional, and therefore, hinder comparisons between strain *shapes* in his model with strain shapes measured in three dimensions (constrictions and flattenings) in natural plutons. However, two-dimensional strain *intensities* and *orientations* in his model can be qualitatively compared with measured strains within and around the Merrimac plutons to limit their level of emplacement. Strains within the northern Merrimac pluton are qualitatively consistent with strain orientation and intensity patterns in Dixon's model in which mushrooming occurred. In both this model and the Northern Merrimac pluton, the shortest axis of the strain ellipsoid is nearly horizontal within and around the pluton (Fig. 6). In addition, the center and the margins of the pluton have higher strains than the region in between these locations (Fig. 8a).

Cruden (1988, 1990) studied strains associated with creeping fluid flow passing a non-expanding sphere. His model simulates pluton rising long distances through the crust and, therefore, corresponds to a more mature stage of pluton emplacement when compared with Dixon's model (Fig. 8b). Cruden's model does not simulate the effect of tectonic deformation or interfering diapirs, therefore, his models can not explain the foliation triple points at the ends of the Merrimac plutons (see section on triple points below). However, the strains around the upper hemisphere of the pluton in Cruden's model are consistent with the strains on the sides of the Merrimac plutons, which suggests that at least part of the strains measured around the Merrimac plutons could be due to flow of country rock around the rising, non-expanding, plutons.

Numerical models also suggest that viscous flow could influence strain patterns both around and within the pluton. Schmeling *et al.* (1988) simulated a fluid sphere rising through a viscous fluid (Fig. 8c). Like Cruden's centrifuge model, the Schmeling *et al.* numerical model simulates a mature diapir wherein drag at the surface of the sphere produces flattening at the margins and constriction at the center of the sphere. These patterns are consistent with the general strain shapes and intensities found in the margins of the Merrimac plutons. The strain ellipsoid orientations modeled by Schmeling, when compared with strain orientations measured within the

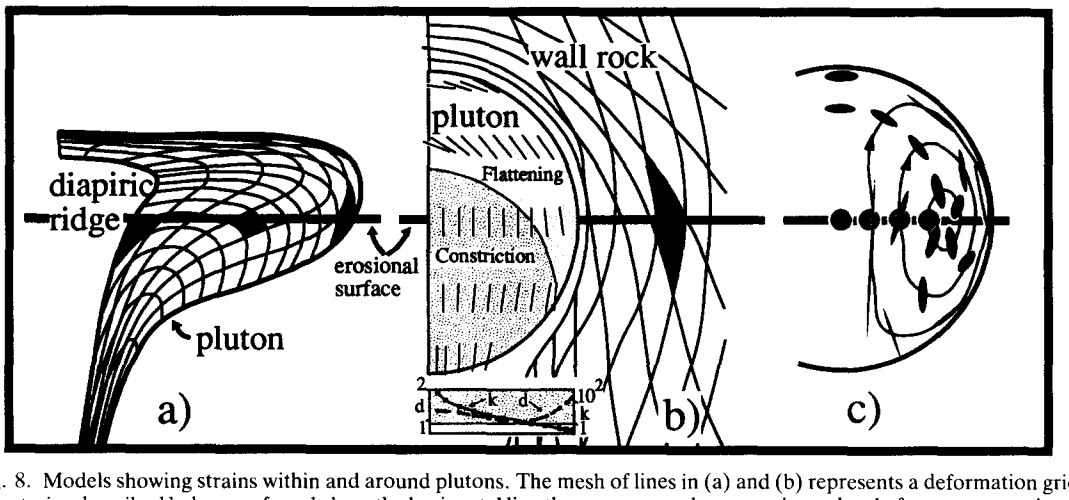

Fig. 8. Models showing strains within and around plutons. The mesh of lines in (a) and (b) represents a deformation grid. The strains described below are found along the horizontal line that represents the approximate level of exposure consistent with the strain's orientation, intensity, and distribution within and around the Merrimac pluton. (a) Black polygons represent two-dimensional shape, orientation and intensities of strain ellipses within the pluton (Dixon 1975); (b) & (c) represent cross-sections of three-dimensional models. (b) Within the pluton (Cruden 1990) see orientation, shape, and intensities of strains in a body that raised two body radii. Strain ellipsoids are vertical (dashes), and shapes vary from constrictional at the center (stippled areas) to flattening at the margin of the pluton (shaded areas). The inset shows values of strain shape k and strain intensity d (Ramsay & Huber 1983). The wall rock (Cruden 1988) shows flattening strains and vertical longer axis of strain ellipsoids around a pluton that raised six body radii. (c) Concentric lines represent flow of magma and black ellipses represent two-dimensional strain ellipsoids within the pluton (Schmelling *et al.* 1989). Strain values are similar to the ones shown in (b).

Merrimac plutons (Figs. 2 and 6), are also consistent with a present erosional surface far below the top of both Merrimac plutons.

However, Schmeling's patterns do not explain the flattening strains measured at the center of the northern Merrimac pluton. Discrepancies between modeled and measured strains can be explained by assumptions in the numerical model, such as the assumption that the Merrimac plutons behaved as a liquid. It is likely that, during progressive crystallization, viscosity within the viscous plutons would gradually increase and cause variations of viscous drag at the pluton's contact. This heterogeneous magma body would produce strain patterns of different shapes from the modeled strain patterns. Furthermore, factors other than viscous drag at the pluton surface probably influenced strain shape of the enclaves within the pluton. Pluton expansion (see above) and thermal convection within the magma chamber could affect the strain patterns within the pluton. In addition, experiments with cooling paraffin (Brandeis & Marsh 1989) show that increasing viscosities may lower convection rates and change convection patterns in a cooling magma. These changes in convection patterns over time and space suggest that measured patterns may differ from the ones in Schmeling's models. However, the origin of flattening enclaves in the center of the northern Merrimac pluton remains unclear.

In summary, the comparison of strain patterns within the Merrimac plutons with the models in Fig. 8 suggest that: (1) the top of the Merrimac plutons is far above the present erosional surface; (2) the strains within the plutons can be explained, in part, by flow of country rock around the rising, non-expanding, pluton; and (3) strains within the plutons can be explained by igneous rather than tectonic processes.

TRIPLE POINTS

Several workers have mapped foliation triple points around plutons (Sylvester 1964, Brun & Pons 1981, Brun *et al.* 1981, 1990, Brun 1983b, Lagarde *et al.* 1990, Pesquera & Pons 1990, Paterson *et al.* 1991). Only Brun *et al.* (1981) and Lagarde *et al.* (1990) documented constrictional strains at triple points. Shapes and intensities of strains in triple points associated with the Merrimac plutons are shown in Figs. 2–6.

Foliation triple points may help eliminate alternative kinematic models for the emplacement of the Merrimac plutons. It is likely that either non-expanding pretectonic or expanding plutons would alter strain fields in the wall rock and form triple points. However, triple points would not form if a pluton emplaces by posttectonic stoping alone. The wrapping of *xy* planes of strain ellipsoids around the pluton, and the presence of foliation triple points (Fig. 2) suggest that the Merrimac plutons deformed the wall rock, in part, by ductile strain.

Brun & Pons (1981) and Brun (1983a) suggested that foliation triple points may be related to pluton expansion in a crust undergoing ductile non-coaxial (bulk simple-shear) deformation. Their computer simulation produced flattening strains on the sides and foliation triple points with constrictional strains at the ends of the pluton. This is the only published model that accounts for the general constrictional triple points measured at the ends of the Merrimac plutons. However, the strains surrounding the Merrimac plutons were not necessarily produced by pluton expansion in a non-coaxial tectonic regime. Three-dimensional computer models (Guglielmo 1992, in press a,b) suggest that pre-, syn- or posttectonic pluton emplacement in both coaxial (bulk pure-shear) and non-coaxial ductile tectonic environments may produce constrictional triple points in map view at the ends of plutons.

Strains around the Merrimac plutons are heterogeneous and were, in part, affected by interactions with neighboring plutons. For example, the positions of the foliation triple points of the southern Merrimac pluton are asymmetric. The distances between this pluton and its triple points are 4 km for the western point and only a few hundred meters for the eastern point (Fig. 2). This asymmetry may be due, in part, to interactions between strain fields of the southern Merrimac pluton and the Cascade and Bald Rock plutons.

Although neighboring plutons probably played a role, the genesis of the strain pattern around the Merrimac plutons also involved tectonic deformation. Regional foliation in this part of the Central Belt of the northern Sierra Nevada follows a NW trend (Hietanen 1983, Dilek 1990). Coincidentally, two lines connecting triple points of each of the Merrimac plutons also define an approximate NW trend (Fig. 2). The alignment of these three structural elements suggests that strains around the Merrimac plutons are not explained by interference with neighboring plutons alone. These strains must also be the result of interactions with strains caused by regional tectonic deformation.

Strains related to the emplacement of the Merrimac plutons contributed significantly to the strains in the wall rock. For example: The triple point west of the southern Merrimac pluton is as far as 4 km (half a body radius) from the pluton. Modeling of pluton expansion and tectonic deformation (Guglielmo 1993) suggests that the width of strain aureole around the pluton must be larger than the distance between pluton and foliation triple point. This is true for pre-, syn- and post-tectonic plutons and for plutons emplaced in either coaxial or non-coaxial tectonic regime. Therefore it is likely that pluton-related strains affected rocks at least 6–8 km from the pluton.

Strain patterns such as those found around the Merrimac plutons may be more common than presently assumed. Despite the immense literature on the structural aspects of plutons, comparatively few studies have actually measured strains associated with pluton emplacement (Holder 1981, Sanderson & Meneilly 1981, Fernandez & Laboue 1983, Courrioux 1987, Fernandez 1987, Ramsay 1989, Brun *et al.* 1990, Lagarde *et al.* 1990, Fowler & Paterson 1991, Paterson *et al.* 1991). There-

fore, it is possible that strain patterns similar to the ones around the Merrimac plutons are common elsewhere in the Sierra Nevada and other orogenic belts. Considering the large number of plutons present in orogenic belts, and the relatively short distances between plutons, the contribution of pluton emplacement dynamics to deformation in country rocks is very significant.

TIME OF EMPLACEMENT RELATIVE TO FORMATION OF WALL ROCK STRUCTURES

Timing of pluton emplacement with respect to regional deformation is difficult to determine unequivocally for the Merrimac plutons or for any other pluton (Paterson & Tobisch 1988). Timing relationships between porphyroblasts formed during contact metamorphism and regional fabrics are commonly used as criteria to establish timing of pluton emplacement (Bell & Rubenach 1983, Vernon 1989a,b). However, the Merrimac plutons are surrounded by ultramafic rocks and marbles in which porphyroblasts are rare and not diagnostic of timing relationships between pluton emplacement and regional cleavage. Other factors contribute to the ambiguity of timing interpretations. For example, a pluton may have post-tectonic structures at its top and syn-tectonic structures at its tail (Hopson *et al.* 1991). Furthermore, forcible post-tectonic intrusions and pre-tectonic plutons commonly produce comparable structures in the wall rock (Noble 1950).

Relationships between wall rock foliations and boundary of the Merrimac pluton are consistent with, but not diagnostic of, post-tectonic pluton emplacement. Wall rock foliations do not cut the pluton's boundary. With exception of eastern part of the southern Merrimac pluton, where the foliation in the wall rock interfingers with the pluton's contact, the foliation in the wall rock is mostly parallel to the boundaries of the pluton (Fig. 2). These relationships are consistent with post-tectonic, forcible, emplacement, however, these relationships are also consistent with pre-tectonic emplacement. Wall rock foliations parallel to the pluton's boundaries could form if a pre-tectonic pluton behaves as a rigid object during subsequent tectonic events and does not record tectonic deformation (e.g. Paterson *et al.* 1987). Nevertheless, this does not seem the case of the Merrimac plutons, which are younger than the early Mesozoic regional deformation. Furthermore, the Merrimac plutons are rich in quartz and biotite. After complete crystallization of the pluton, these minerals would easily record at least some of the strong regional deformation (Fig. 2) that created the structures in the country rock. Therefore, the absence of tectonic strains within the Merrimac plutons is consistent with post- or, at most, very late syn-tectonic final crystallization for both Merrimac plutons, and, at the present level of exposure, the age of the Merrimac plutons provides an upper limit for the age of the structures in the country rocks of the Central Belt of northern Sierra Nevada.

Age of plate subduction

Rocks around the Merrimac plutons have been interpreted as mélange (Schweickert & Cowan 1975, Edelman *et al.* 1989, Edelman & Sharp 1989). These rocks are thought to have formed during a late Triassic to early Jurassic subduction along the western edge of the North American plate (Schweickert & Cowan 1975, Edelman *et al.* 1989). The time of subduction was established by using cross-cutting relationships between plutons of known ages (Evernden & Kistler 1970, Lamphere & Reed 1973) with structures in the Central Belt. However, strains and structures associated with plutons in the northern Sierra Nevada have not been studied in detail. Therefore, it is possible that plutons used to determine the age of the Central Belt are composed of several independent intrusions like the Merrimac, some of which may even be pre-tectonic. These uncertainties leave open the upper limit for the age of the Triassic (?) subduction along the Cental Belt. The strain patterns presented herein provide the first strain measurements associated with pluton emplacement in the northern Sierra Nevada. They suggest that both the Merrimac plutons crystallized after or, at most, during the formation of the structures in the country rock. Therefore, U/Pb ages of these plutons (142 $\pm$ 3 Ma) contribute to place a more reliable upper limit on the age of the cleavage associated with the Triassic(?) subduction.

CONCLUSIONS

This paper reports and analyzes strain measurements within and around the Merrimac pluton in northern Sierra Nevada. The main conclusions are: (1) expansion in the Merrimac plutons did not occur in the solid state; (2) strain within the Merrimac plutons is caused by igneous rather than tectonic processes; (3) the Merrimac plutons contributed significantly to the ductile strains observed in the wall rock; and (4) the Merrimac plutons were emplaced after or during the formation of regional structures.

Acknowledgements—This work was supported by National Science Foundation grant EAR-8904706, GSA grant 4213-89, and Sigma Xi, and AGI grants. I would like to thank Othmar Tobisch, Casey Moore, Ken Collerson, Dan Schultz-Ela, Scott Paterson, Art Sylvester and Steven Wojtal for comments that greatly improved the manuscript.

REFERENCES

Balk, R. 1937. The structural behavior of igneous rocks. *Mem. geol. Soc. Am.* **5**, 177.

Barton, M. D. & Hanson, R. B. 1989. Magmatism and the development of low-pressure metamorphic belts: implications from the western United States and thermal modeling. *Bull. geol. Soc. Am.* **101**, 1051–1065.

Bateman, P. C. & Clark, L. D. 1974. Stratigraphic and structural setting of the Sierra Nevada Batholith, California. *Pacific Geol.* **8**, 79–89.

Bell, T. H. & Rubenach, M. J. 1983. Sequential porphyroblast growth and crenulation cleavage developed during progressive deformation. *Tectonophysics* **92**, 171–194.

Berger, R. R. & Pitcher, W. S. 1970. Structures in granite rocks: a commentary and a critique on granite tectonics. *Proc. Geol. Ass.* **81**, 441–461.

Bickford, M. E. & Day, H. W. 1988. Jurassic ages of arc–ophyolite complexes, Northern Sierra Nevada: Implications for duration of the Nevadan "orogeny". *Geol. Soc. Am. Abs. w. Prog.* **20**, 274.

Bottinga, Y. & Weill, D. F. 1972. The viscosity of magmatic silicate liquids: A model for calculation. *Am. J. Sci.* **272**, 438–475.

Brandeis, G. & Marsh, B. D. 1989. The convective liquidus in a solidifying magma chamber: a fluid dynamic investigation. *Nature* **339**, 613–616.

Brun, J.-P. 1983a. Isotropic points and lines in strain fields. *J. Struct. Geol.* **5**, 321–327.

Brun, J.-P. 1983b. L'origine des dômes gneissiques: modeles et tests. *Bull. Soc. géol. Fr.* **7**, 219–228.

Brun, J.-P., Gapais, D. & Le Theoff, B. 1981. The mantled gneiss domes of Kuopio (Finland): interferring diapirs. *Tectonophysics* **74**, 283–304.

Brun, J.-P., Gapais, D. & Cogne, J.-P. 1990. The Flamaville Granite (Northwest France): an unequivocal example of a syntectonically expanding pluton. *Geol. J.* **25**, 271–286.

Brun, J.-P. & Pons, J. 1981. Strain patterns of pluton emplacement in a crust undergoing non-coaxial deformation, Sierra Morena, Southern Spain. *J. Struct. Geol.* **3**, 219–230.

Clark, L. D. 1976. Stratigraphy of the north half of the western Sierra Nevada metamorphic belt. *Prof. Pap. U.S. geol. Surv.* **923**, 26.

Courrioux, G. 1987. Oblique diapirism: the Criffel granodiorite/granite zoned pluton (southwest Scotland). *J. Struct. Geol.* **9**, 313–330.

Cruden, A. R. 1988. Deformation around a rising diapir modeled by creeping flow past a sphere. *Tectonics* **7**, 1091–1101.

Cruden, A. R. 1990. Flow and fabric development during the diapiric rise of magma. *J. Geol.* **98**, 681–698.

Day, H. W., Moores, E. M. & Tuminas, A. C. 1985. Structure and tectonics of the northern Sierra Nevada. *Bull. geol. Soc. Am.* **96**, 436–450.

Day, H. W., Schiffman, P. & Moores, E. M. 1988. Metamorphism and tectonics of the northern Sierra Nevada. In: *Metamorphism and Crustal Evolution of the Western United States—Rubey Volume* (edited by Ernst, W. G.). *Am. Geophys. Un. Geophys. Monogr.* **7**, 736–763.

Dilek, Y. 1989. Structure and tectonics of an Early Mesosoic oceanic basement in the northern Sierra Nevada metamorphic belt, California—evidence for transform faulting and ensimatic arc evolution. *Tectonics* **8**, 999–1014.

Dilek, Y., Thy, P. & Moores, E. M. 1991. Episodic dike intrusions in the northwestern Sierra Nevada, California—implications for multistage evolution of a Jurassic arc terrane. *Geology* **19**, 180–184.

Dixon, J. M. 1975. Finite strain and progressive deformation in models of diapiric structures. *Tectonophysics* **28**, 89–124.

Dunnet, D. 1969. A technique of finite strain analysis using elliptical particles. *Tectonophysics* **7**, 117–136.

Edelman, S. H., Day, H. W., Moores, E. M., Zigan, S. M., Murphy, T. P. & Hacker, B. R. 1989. Structure across a Mesozoic ocean–continent suture zone in the northern Sierra Nevada, California. *Spec. Pap. geol. Soc. Am.* **224**, 56.

Edelman, S. H. & Sharp, W. D. 1989. Terranes, early faults, and pre-Late Jurassic amalgamation of the western Sierra Nevada metamorphic belt, California. *Bull. geol. Soc. Am.* **101**, 1420–1433.

Escorza, C. M. 1978. Estructura y deformación de los enclaves microgranulares negros (gabarros) del Alto de los Leones, Guadarrama. *Bol. R. Soc. Española Hist. Nat.* **76**, 57–87.

Etheridge, M. A., Wall, V. J. & Vernon, R. H. 1983. The role of the fluid phase during regional metamorphism and deformation. *J. metamorph. Geol.* **1**, 205–226.

Evernden, J. F. & Kistler, R. W. 1970. Chronology of emplacement of Mesozoic batholithic complexes in California and western Nevada. *Prof. Pap. U.S. geol. Surv.* **623**, 42.

Fernandez, A. 1987. Structural petrology and intrusion strain analysis. *Rev. Brasil. Geosci.* **17**, 372–381.

Fernandez, A. & Laboue, M. 1983. Développement de l'orientation préférentielle de marqueurs rigides lors d'une déformation par aplatissement de révolution. Étude théorique et application aux structures de mise en place du granite de la Margeride au voisinage du bassin du Malzieu (Massif Central français). *Bull. Soc. geol. Fr.* **7**, 327–334.

Fowler, T. K., Jr. & Paterson, S. R. 1991. On the role of ductile wall rock deformation during emplacement: Constrains from quantitative strain analysis. *Geol. Soc. Am. Abs. w. Prog.* **23**, 26.

Grommé, C. S., Merril, R. T. & Verhoogen, J. 1967. Paleomagnetism of Jurassic and Cretaceous plutonic rocks in the Sierra Nevada, California, and its significance for polar wandering and continental drift. *J. geophys. Res.* **72**, 5661–5684.

Guglielmo, G., Jr. 1992. 3-D computer graphics in modeling pluton emplacement. In: *Computer Graphics in Geology* (edited by Pflug, R. & Harbaugh, J. W.). *Lecture Notes in Earth Sciences, Vol.* 41. Springer, New York, 171–185.

Guglielmo, G., Jr. In press a. Interference between pluton expansion and non-coaxial deformation: three-dimensional computer model and field implications. *J. Struct. Geol.* **15**.

Guglielmo, G., Jr. In press b. Nested plutons as geopetal structures: The Merrimac plutons, northern Sierra Nevada, California. *Geol. J.*

Guglielmo, G., Jr. In press c. Interference between pluton expansion and coaxial tectonic deformation: three-dimensional computer model and field implications. *J. Struct. Geol.*

Hietanen, A. 1951. Metamorphic and igneous rocks of the Merrimac Area. Plumas National Forest, California. *Bull. geol. Soc. Am.* **67**, 565–607.

Hietanen, A. 1973. Geology of the Pulga and Bucks Lake quadrangles, Butte and Plumas counties, California. *Prof. Pap. U.S. geol. Surv.* **731**, 66.

Hietanen, A. 1976. Metamorphism and plutonism around the middle and south forks of the Feather River, California. *Prof. Pap. U.S. geol. Surv.* **920**, 30.

Hietanen, A. 1981. Petrologic and structural studies in the northwestern Sierra Nevada, California. *Prof. Pap. U.S. geol. Surv.* **1226**, 59.

Holder, M. T. 1979. An emplacement mechanism for post-tectonic granites and its implications for their geochemical features. In: *Origin of Granite Batholiths—Geochemical Evidence* (edited by Atherton, M. P. & Tarney, J.). Shiva Publishing, Orpington, 116–128.

Holder, M. T. 1981. Some aspects of intrusion of ballooning: the Ardara pluton. *J. Struct. Geol.* **3**, 89–95.

Hopson, C. A, Dellinger, D. A. & Mattinson, J. M. 1991. Granitoid diapir tectonics and petrogenesis, north Cascades, WA. *Geol. Soc. Am. Abs. w. Prog.* **23**, 36.

Hsu, T. C. 1966. The characteristics of coaxial and non coaxial strain paths. *J. Strain Anal.* **1**, 216–222.

Hutton, D. 1982. A tectonic model for the emplacement of the main Donegal granite, NW Ireland. *J. geol. Soc. Lond.* **139**, 615–631.

Jackson, M. P. A. & Talbot, C. J. 1989. Anatomy of mushroom-shaped diapirs. *J. Struct. Geol.* **11**, 211–230.

Jennings, C. W., Stand, R. G. & Rogers, T. H. 1973. *Geological Map of California*, scale 1:750,000. Division of Mines and Geology, California Geologic Data Map Series.

Koyi, H. 1991. Mushroom diapirs penetrating overburdens with high effective viscosities. *Geology*, **19**, 1229–1232.

Lagarde, J. L. & Choukroune, P. 1982. Cisaillement ductile et granitoides syntectoniques: l'exemple du massif hercynien des Jebilets. *Bull. Soc. géol. Fr.* **7**, 299–307.

Lagarde, J. L., Omar, S. A. & Rodaz, B. 1990. Structural characteristics of granitic plutons emplaced during weak regional deformation: examples from late Carboniferous plutons, Morocco. *J. Struct. Geol.* **12**, 805–821.

Lanphere, M. A. & Reed, B. L. 1973. Timing of Mesozoic and Cenozoic plutonic events in circum-Pacific North America. *Bull. geol. Soc. Am.* **84**, 3773–3782.

Lisle, R. J. 1977. Clastic grain shape and orientation in relation to cleavage from Aberystwyth grits, Wales. *Tectonophysics* **12**, 307–325.

Lode, W. 1926. Versuche uber den Einfluss der mittleren Hauptspannung auf das fliessen des Matalle Eisen, Kupfer, and Nickel. *Z. Phys.* **36**, 913–939.

Marre, J. 1987. *The Structural Analyses of Granitic Rocks.* Elsevier, New York.

Marsh, B. D. 1982. On the mechanics of igneous diapirism, stoping and zone melting. *Am. J. Sci.* **282**, 808–855.

Mazaheri, S. A. 1982. The petrology and metamorphism of ultramafic and mafic rocks near Pulga, Butte County, California. Unpublished Ph.D. thesis, University of California, Davis.

Miller, D. M. & Oertel, G. 1979. Strain determination from the measurement of pebble shapes: a modification. *Tectonophysics* **55**, T11–T13.

Murphy, T. P. 1986. Stratigraphy and structure of the Clipper Mills area, northern Sierra Nevada, California. Unpublished M.Sc. thesis, University of California, Davis.

Murphy, T. P. & Moores, E. M. 1985. Two ophiolitic, tectonostratigraphic terranes in the western Central Belt, northern Sierra Nevada, California. *Geol. Soc. Am. Abs. w. Prog.* **17**, 372.

Nadai, A. 1963. *Theory of Flow and Fracture of Solids*. Engineering Societies Monographs. McGraw-Hill, New York.

Noble, J. A. 1950. Evaluation of criteria for the forcible intrusion of magma. *J. Geol.* **60**, 34–57.

Paterson, S. R. & Tobisch, O. T. 1988. Using pluton ages to date regional deformation: Problems with present criteria. *Geology* **16**, 1108–1111.

Paterson, S. R., Tobisch, O. T. & Saleeby, J. B. 1987. Recognition of pre-tectonic intrusives: implications for the dating of structural events. *Geol. Soc. Am. Abs. w. Prog.* **19**, 800.

Paterson, S. R., Tobisch, O. T. & Vernon, R. H. 1991. Emplacement and deformation of granitoids during volcanic arc construction in the Foothills terrane, central Sierra Nevada, California. *Tectonophysics* **191**, 89–110.

Paterson, S. R., Vernon, R. H. & Tobisch, O. T. 1989. A review of the criteria for the identification of magmatic and tectonic foliations in granitoids. *J. Struct. Geol.* **11**, 349–363.

Pesquera, A. & Pons, J. 1990. Le pluton hercynien de Aya (Pyrénées basques espagnoles). Structure, mise en place et incidences tectoniques régionales. *Bull. Soc. géol. Fr.* **8**, 13–21.

Ramberg, H. 1970. Model studies in relation to intrusion of plutonic bodies. In: *Mechanism of Igneous Intrusion*. Gallery Press, Liverpool.

Ramberg, H. 1972. Theoretical models of density stratification and diapirism in the earth's crust. *J. geophys. Res.* **77**, 877–889.

Ramberg, H. 1981. *Gravity Deformation of the Earth's Crust. Theory, Experiments, and Geological Application*. Academic Press, London.

Ramsay, J. G. 1975. The structure of the Chindamora batholith. *19th Ann. Rep. Res. Inst. Afr. Geol., Univ. Leeds* **81**.

Ramsay, J. G. 1989. Emplacement kinematics of a granite diapir: the Chindamora batholith, Zimbabwe. *J. Struct. Geol.* **11**, 191–209.

Ramsay, J. G. & Huber, M. I. 1983. *The Techniques of Modern Structural Geology, Volume* 1: *Strain Analysis*. Academic Press, London.

Sanderson, D. J. & Meneilly, A. W. 1981. Analysis of three-dimensional strain modified uniform distributions: andalusite fabrics from a granite aureole. *J. Struct. Geol.* **3**, 109–116.

Schmeling, H., Cruden, A. R. & Marquart, G. 1988. Finite deformation in and around a fluid sphere moving through a viscous medium: implications for diapiric ascent. *Tectonophysics* **149**, 17–34.

Schweickert, R. A. 1978. Triassic and Jurassic paleogeography of the Sierra Nevada and adjacent regions, California and western Nevada. In: *Mesozoic Paleogeography of the Western United States, Pacific Coast Paleogeography Symposium, Vol.* 2 (edited by Howell, D. G. & McDougall, K. A.). Society of Economic Paleontologists and Mineralogists, Bakersfield, 361–384.

Schweickert, R. A. & Cowan, D. S. 1975. Early Mesozoic tectonic evolution of the western Sierra Nevada, California. *Bull. geol. Soc. Am.* **86**, 1329–1336.

Schweickert, R. A., Bogen, N. L., Girty, G. H., Hanson, R. E. & Merguerien, C. 1984. Timing and structural expression of the Nevadan orogeny, Sierra Nevada, California. *Bull. geol. Soc. Am.* **95**, 967–979.

Schwerdtner, W. M., Bennett, P. J. & James, W. T. 1977. Application of *L–S* fabric scheme to structural mapping and paleostrain analysis. *Can. J. Earth Sci.* **14**, 1021–1032.

Schwerdtner, W. M. & Troeng, B. 1978. Strain distribution within arcuate diapiric ridges of silicone putty. *Tectonophysics* **50**, 13–28.

Sharp, W. D. 1988. Pre-Cretaceous crustal evolution in the Sierra Nevada region, California. In: *Metamorphism and Crustal Evolution of the Western United States* (edited by Ernst, W. G.). Prentice-Hall, Englewood Cliffs, New Jersey, 823–864.

Shaw, H. R. 1965. Comments on viscosity, crystal settling, and convection in granite magmas. *Am. J. Sci.* **263**, 120–152.

Shimamoto, I. & Ikeda, Y. 1976. A simple algebraic method for strain estimation from deformed ellipsoidal objects. 1. Basic theory. *Tectonophysics* **36**, 315–337.

Soula, J. C. 1982. Characteristics and mode of emplacement of gneiss domes and Plutonic domes in central-eastern Pyrenees. *J. Struct. Geol.* **4**, 313–342.

Sylvester, A. G. 1964. The Precambrian rocks of the Telemark area in south central Norway. III—Geology of the Vrådal granite. *Norsk Geologisk Tidsskrift* **44**, 445–482.

Talbot, C. J. 1974. Fold nappes as asymmetric mantled gneiss domes and ensialic orogeny. *Tectonophysics* **24**, 259–276.

Talbot, C. J. 1977. Inclined asymmetric upward-moving gravity structures. *Tectonophysics* **42**, 159–181.

Taliaferro, N. L. 1942. Geologic history and correlation of the Jurassic of southwestern Oregon and California. *Bull. geol. Soc. Am.* **53**, 71–112.

Tobisch, O. T., Saleeby, J. B. & Fiske, R. S. 1986. Structural history of continental volcanic arc rocks, eastern Sierra Nevada, California: a case of extensional tectonics. *Tectonics* **1**, 65–94.

Van der Molen, I. & Paterson, M. S. 1979. Experimental deformation of partially melted granite. *Contr. Miner. Petrol.* **70**, 299–318.

Vernon, R. H. 1989a. Evidence of syndeformational contact metamorphism from porphyroblast–matrix relationships. *Tectonophysics* **158**, 113–126.

Vernon, R. H. 1989b. Porphyroblast–matrix microstructural relationships—Recent approaches and problems. In: *The Evolution of Metamorphic Belts* (edited by Daly, S. J. & Brown, M.). *Spec. Publs geol. Soc. Lond.* **43**, 83–102.

Vernon, R. H., Etheridge, M. A. & Wall, V. C. 1988. Shape and microstructure of microgranitoid enclaves: indicators of magma mingling and flow. *Lithos* **22**, 1–11.